

Modeling the Yildiz Motor revisited

Citation for published version (APA):

Duarte, J. L. (2018). *Modeling the Yildiz Motor revisited*. <https://doi.org/10.6100/6b67487a-bd78-4a24-bdd1-d7b9b3dbd5b7>

DOI:

[10.6100/6b67487a-bd78-4a24-bdd1-d7b9b3dbd5b7](https://doi.org/10.6100/6b67487a-bd78-4a24-bdd1-d7b9b3dbd5b7)

Document status and date:

Published: 22/07/2018

Document Version:

Accepted manuscript including changes made at the peer-review stage

Please check the document version of this publication:

- A submitted manuscript is the version of the article upon submission and before peer-review. There can be important differences between the submitted version and the official published version of record. People interested in the research are advised to contact the author for the final version of the publication, or visit the DOI to the publisher's website.
- The final author version and the galley proof are versions of the publication after peer review.
- The final published version features the final layout of the paper including the volume, issue and page numbers.

[Link to publication](#)

General rights

Copyright and moral rights for the publications made accessible in the public portal are retained by the authors and/or other copyright owners and it is a condition of accessing publications that users recognise and abide by the legal requirements associated with these rights.

- Users may download and print one copy of any publication from the public portal for the purpose of private study or research.
- You may not further distribute the material or use it for any profit-making activity or commercial gain
- You may freely distribute the URL identifying the publication in the public portal.

If the publication is distributed under the terms of Article 25fa of the Dutch Copyright Act, indicated by the "Taverne" license above, please follow below link for the End User Agreement:

www.tue.nl/taverne

Take down policy

If you believe that this document breaches copyright please contact us at:

openaccess@tue.nl

providing details and we will investigate your claim.

Modeling the Yildiz Motor revisited

J.L. Duarte

Department of Electrical Engineering
Eindhoven University of Technology
The Netherlands

Abstract

With regard to classical Electromagnetic Theory, a purely analytical approach is followed for describing incommensurable forces arising out of magnetic attraction/repulsion.

1 Introduction

Similar to electric machines, the mechanical device described in [1] consists of an assembly of stationary and moving parts made of non-magnetic material like aluminum or plastic. In both parts permanent magnets are inserted following prescribed geometrical patterns. The inventor claims in [1] that the device is a prime mover "*on its own*", able to unfold mechanical energy without recurrence to other energy sources. Although not all constituting parts of the apparatus have yet been fully disclosed, a few experiments with working prototypes indicate that the claims should be at least not prematurely discarded [2].

Recently, while searching for energy harvesting opportunities and motivated by the ideas in [1], the authors in [3] have noticed that, by introducing excentric displacements in permanent magnet structures similar to the ones in [1], an incommensurable torque can be perceived by numerical calculations with FEM.

On account of analytical formulations only, and backed by interpretations of main-stream theories in Physics, the model presented in the following sections attempts describing in its simplest form the fundamental behaviour of the prime mover as claimed by [1]. The model is easy to understand, therefore easy to be falsified by an interested reader.

[HTTPS://DOI.ORG/10.6100/6B67487A-BD78-4A24-BDD1-D7B9B3DBD5B7](https://doi.org/10.6100/6B67487A-BD78-4A24-BDD1-D7B9B3DBD5B7)

2 Magnetic forces acting on current loops

A magnetic force originates from and acts upon electrical charges possessing a velocity. The magnetic force \vec{F} which acts on an electrical charge q moving with velocity \vec{v} in the magnetic field \vec{B} is given by [4]

$$\vec{F} = q\vec{v} \times \vec{B}, \quad (1)$$

while an electrical charge q moving with velocity \vec{v} will produce a magnetic field \vec{B} around itself as

$$\vec{B} = \frac{\mu_0}{4\pi} q \frac{\vec{v} \times \vec{r}}{r^3}, \quad (2)$$

where \vec{r} is the vector from the charge to the field point, and μ_0 is the electromagnetic intrinsic inductance per unity length of free space, with $\mu_0 = 4\pi \times 10^{-7} [H/m]$.

On account of (1) and (2), the interaction of magnetic forces between currents is formulated as a law of forces acting between two infinitesimal current elements at a given distance from each other and having a given orientation with respect to one other [5].

Consider two filamentary circular current loops (primary and secondary) as sketched in Fig. 1, with inner radii R_P and R_S and constant currents I_P and I_S ,

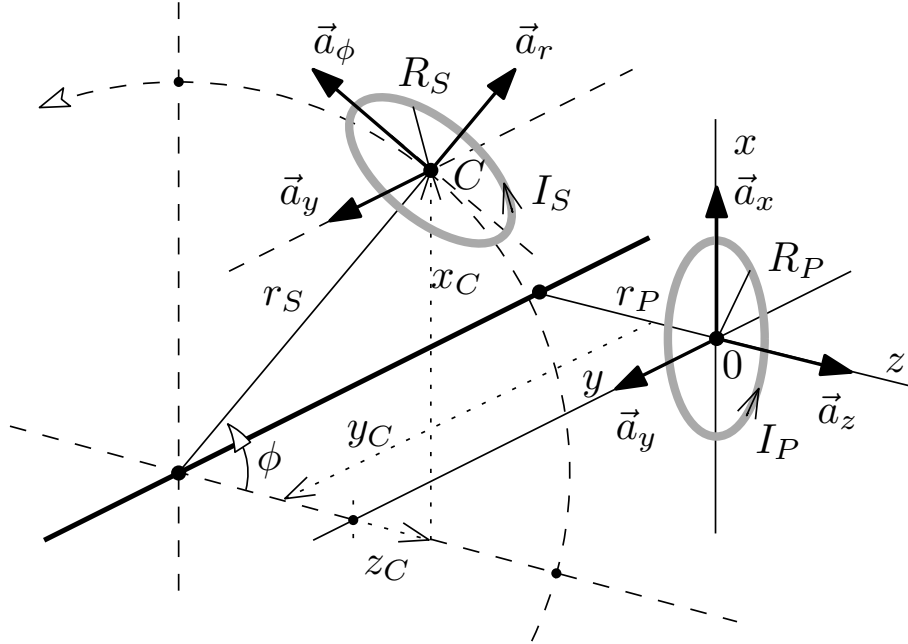


Fig. 1: Circular current loops with angular misalignment. The primary loop is fixed, the secondary can translate around a pivot axis.

respectively. The center of the primary loop is located at the origin of a cartesian system (x, y, z) characterized by the unity vectors

$$\vec{a}_x = \vec{a}_y \times \vec{a}_z, \vec{a}_y = \vec{a}_z \times \vec{a}_x, \vec{a}_z = \vec{a}_x \times \vec{a}_y, \quad (3)$$

with \vec{a}_z normal to the loop plane. The secondary loop can have circumferential translational movement with constant radius, r_S , perpendicular to a pivot line parallel to the y -axis, and with turning point at coordinates $(x = 0, y = y_C, z = -r_P)$. The secondary loop plane is tangential to the translational trajectory, from which the inclination is characterized by the angle ϕ referenced to the z -axis.

By observation of Fig. 1 it is possible to derive that the secondary loop has center at $C(x_C, y_C, z_C)$, where

$$x_C = r_S \sin \phi, \quad (4)$$

$$z_C = r_S \cos \phi - r_P, \quad (5)$$

and y_C may be freely chosen. The associated normal and tangential unity vectors to the secondary loop are found to become

$$\vec{a}_r = \sin \phi \vec{a}_x + \cos \phi \vec{a}_z, \quad (6)$$

$$\vec{a}_\phi = \cos \phi \vec{a}_x - \sin \phi \vec{a}_z, \quad (7)$$

respectively, with $\vec{a}_r = \vec{a}_\phi \times \vec{a}_y$, $\vec{a}_\phi = \vec{a}_y \times \vec{a}_r$, $\vec{a}_y = \vec{a}_r \times \vec{a}_\phi$.

For given inclination ϕ and pivot location y_C , the resulting magnetic forces actuating on the secondary loop can be determined through fully analytical equations [6]. In Appendix A a detailed derivation is given for these force components, found to be

$$\vec{F}_S = F_x \vec{a}_x + F_y \vec{a}_y + F_z \vec{a}_z \quad (8)$$

where F_x , F_y and F_z are calculated with the formula (27) in Appendix A. Alternatively,

$$\vec{F}_S = F_r \vec{a}_r + F_y \vec{a}_y + F_\phi \vec{a}_\phi, \quad (9)$$

where the radial and translational force components with respect to the pivot axis are given by

$$F_r = F_x \sin \phi + F_z \cos \phi, \quad (10)$$

$$F_\phi = F_x \cos \phi - F_z \sin \phi \quad (11)$$

respectively. So, F_y is the axial force along the pivot axis, and the torque around it becomes

$$\vec{T}_S = F_\phi r_S \vec{a}_y. \quad (12)$$

3 Energy excess ?!

The intention now is to explore the energy requirements to translate the secondary loop around the pivot axis ($0 \leq \phi \leq 2\pi$ in Fig. 1), when the axial position of the turning point, i.e. coordinate y_C , is simultaneously allowed to vary as function of the inclination ϕ [3].

For instance, let's impose that the turning point (therefore the coordinates of the loop center) moves in synchronism with the inclination ϕ according to

$$x_C = r_S \sin \phi, \quad (13)$$

$$y_C = A_0 + A_S \sin \theta, \text{ with } \theta = \phi, \quad (14)$$

$$z_C = r_S \cos \phi - r_P, \quad (15)$$

where A_0 is an offset and A_S the amplitude of the axial harmonic displacement of the turning point, which is made synchronized with the changes in x_C and z_C given by (4) and (5).

By assuming infinitesimal increments $\delta\phi$, in the limit sense the energy incrementals introduced by the circumferential and axial forces in (9) are

$$\delta Q_\phi = F_\phi r_S \delta\phi, \quad (16)$$

$$\delta Q_y = F_y \delta y_C = F_y A_S \cos \phi \delta\phi, \quad (17)$$

respectively. The integration of these energy incrementals yields Q_Σ , the total energy necessary to realize one single joint circumferential and longitudinal cycles of the secondary loop, as given by

$$Q_\Sigma = Q_\phi + Q_y, \quad (18)$$

where, in view of (16) and (17),

$$Q_\phi = \int_0^{2\pi} F_\phi r_S d\phi, \quad (19)$$

$$Q_y = \int_0^{2\pi} F_y A_S \cos \phi d\phi. \quad (20)$$

Fig. 2 illustrates the forces F_ϕ and F_y as function of the inclination ϕ , on account of the loop parameters in Table 1. Also, the corresponding values of the energy derivatives

$$\frac{dQ_\phi}{d\phi}, \frac{dQ_y}{d\phi}, \text{ and } \frac{dQ_\Sigma}{d\phi}$$

are shown in Fig. 3. A surprising numerical result is obtained for the total energy involved in Fig. 3, namely

$$Q_\phi = -0.7420 \text{ nJ} ; Q_y = 1.0131 \text{ nJ} ; \quad (21)$$

$$Q_\Sigma = 0.2711 \text{ nJ}. \quad (22)$$

Tab. 1: Parameters and geometrical dimensions of the current loops

Parameter	Value	Description
I_P	[A] -1.0	Current primary loop
I_S	[A] 1.0	Current secondary loop
R_P	[mm] 5.0	Inner radius prim loop
R_S	[mm] 5.0	Inner radius sec loop
r_P	[mm] 30.0	Distance prim loop to pivot axis
r_S	[mm] 25.0	Translational radius of sec loop
A_0	[mm] 9.5	Offset position of turning point
A_S	[mm] 17.0	Amplitude longitudinal motion sec loop

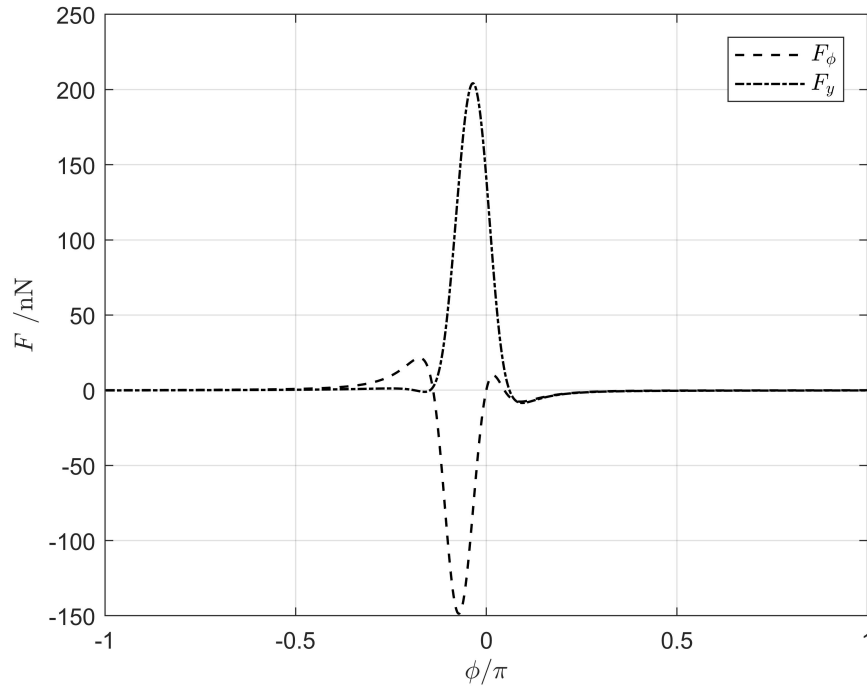


Fig. 2: Illustration of the translational and axial forces during the joint trajectory of the secondary loop around and along the pivot axis, on account of the parameters in Table 1.

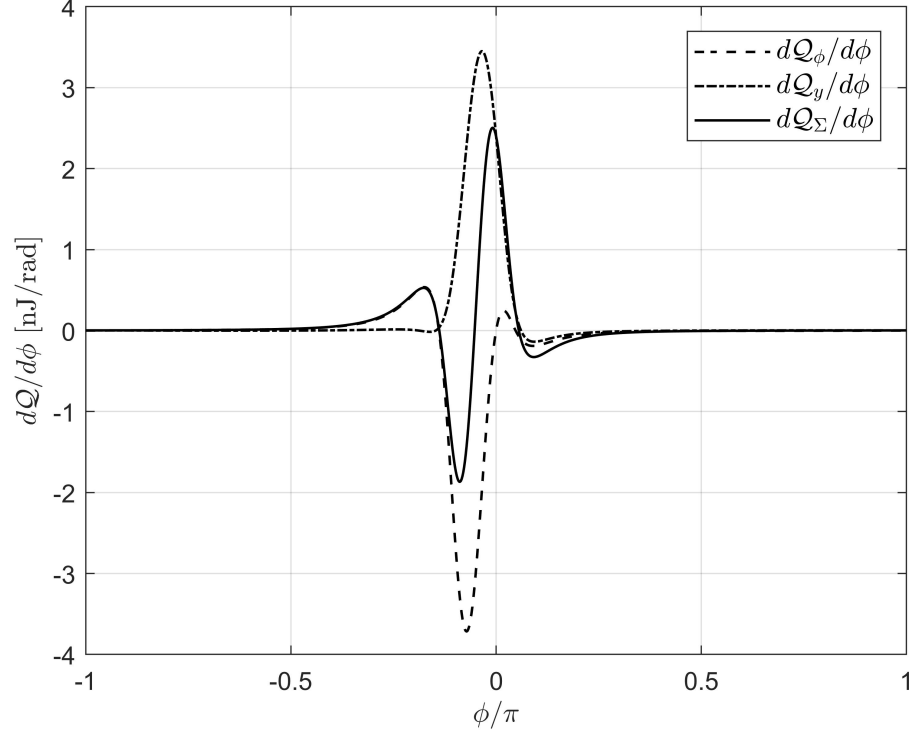


Fig. 3: Translational and axial energy derivatives during the trajectory of the secondary loop around and along the pivot axis ($\theta \equiv \phi$).

So, after one translation of the secondary loop around the pivot axis, an energy *excess* remains ($Q_\Sigma > 0$)

In order to quantify the quality of the numerical results above, Fig. 4 and Fig. 5 show the energy incrementals when translation is performed without axial displacement of the turning point ($0 \leq \phi \leq 2\pi$ and $\theta \equiv 0$), or with axial displacement of the turning point without circular translation of the loop ($\phi \equiv 0$ and $0 \leq \theta \leq 2\pi$), on account of the same parameters in Table 1. For the first situation follows

$$Q_\phi = -3.0371 \times 10^{-16} \text{ nJ} ; Q_y = 0 \text{ nJ} ; \quad (23)$$

$$Q_\Sigma = -3.0371 \times 10^{-16} \text{ nJ} ; \quad (24)$$

A Matlab script is given in Appendix B for the interested reader who would like to check the validity of the performed calculations.

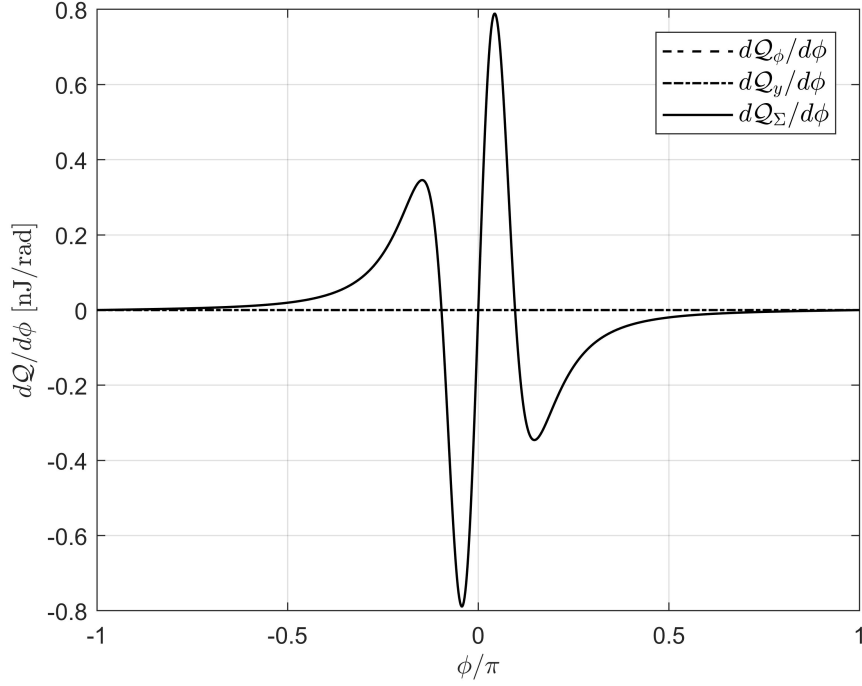


Fig. 4: Translational energy derivatives when the trajectory of the sec loop is around the pivot axis without axial displacement of the turning point ($\theta \equiv 0$).

and for the latter

$$\mathcal{Q}_\phi = -7.3479 \times 10^{-16} \text{ nJ} ; \mathcal{Q}_y = -1.4171 \times 10^{-13} \text{ nJ} ; \quad (25)$$

$$\mathcal{Q}_\Sigma = -1.4245 \times 10^{-13} \text{ nJ}. \quad (26)$$

As expected for both cases, virtually no energy excess appears, since $\mathcal{Q}_\Sigma \approx 0$ in (24) and (26) if compared to (22), up to the numerical precision of the used software.

As a result of the back-and-forward axial movement according to (14), in conjunction with the choosen geometrical parameters in Table 1, the axial force F_y acting on the secondary current loop is predominantly positive (repulsion) when positive incremental displacements of the turning point occurs along the pivot axis ($-\pi/2 < \phi < \pi/2$). In the range where negative incremental displacements of the turning point take place (return path), the axial force is negligible (that is to say, barely axial attraction), as shown in Fig. 3. As a result, the energy incrementals

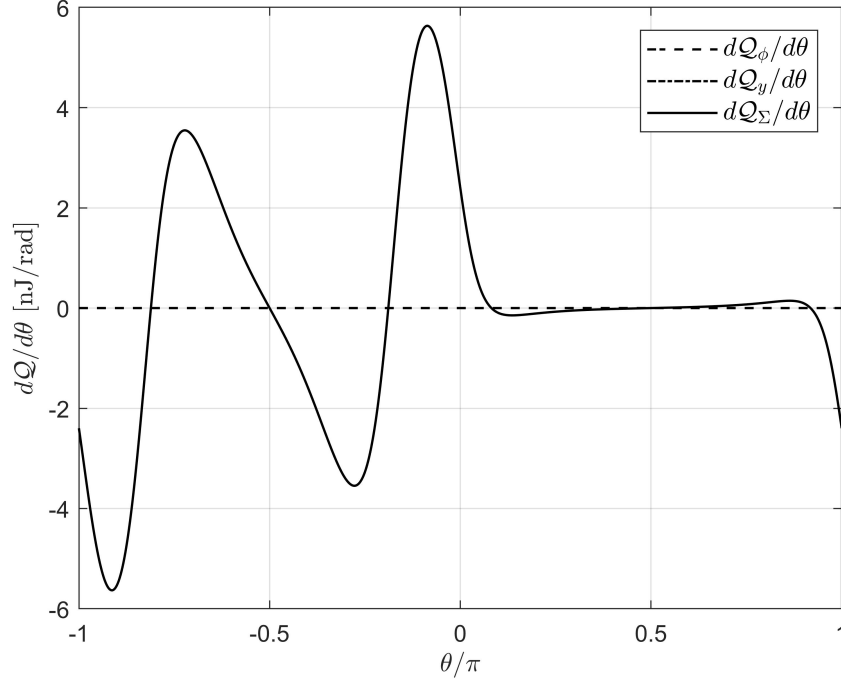


Fig. 5: Axial energy derivatives when the trajectory of the sec loop is along the pivot axis without translational movement ($\phi \equiv 0$).

δQ_y in (17) are predominantly positive.

On the other hand, although the circumferential force F_ϕ in Fig. 3 is on average negative (leading therefore to an average attraction torque between the loops), the resulting energy summation Q_ϕ , due to the translational displacements, is not high enough to fully compensate for the energy injected by the axial force F_y , leading to energy excess after one turn around of ϕ .

The interpretation of the result in (22) is quite appealing. Depending on the angular inclination of the secondary loop, there will be repulsive (positive sign) or attractive (negative sign) forces between the loops. In order to perform one rotation (from 0 to 2π radians) of the moving parts whereon the secondary coil is expected to be assembled (a physical rotor), and, at the same time, to move the rotor back-and-forth along the pivot axis, it is necessary to impose on average a positive axial force to inject 1.0131 nJ into the system. We get back 0.7420 nJ (negative sign) due to the tangential force on the rotor.

So, on account of the interaction of forces between the loops, in total $Q_\Sigma = 0.2711 \text{ nJ}$ is transferred to the inertia of the moving parts by completing one turn

around. After that, the rotor can be released since its inertia will be repeatedly accelerated *on its own* due to the taken-in energy excess ($Q_{\Sigma} > 0$). If friction is present, the rotor will stabilize at the rotational/axial velocities corresponding to the dissipation of $0.2711 nJ$ per revolution.

In the next section an argumentation is made for a possible source of energy that would make the outcomes above in agreement with main-stream theories in Physics.

4 Free Space as a source of energy in abundance

A circular current loop in a plane, as in Fig. 1, creates a magnetic moment with magnitude equal to the current multiplied by the area enclosed by the current contour and direction the same as the normal to the surface. Magnetic moments are the atomic source of magnetism [4].

The permanent magnet acquires its magnetic properties owing to the orbital circulation and rotation of electrons, which creates magnetic moments per unit volume of material, also called magnetization. Quite peculiar, the permanent magnet is characterized by the property that its constituent magnetic moments are all aligned in the same direction, and that the atomic motion of electrons is non-dissipative [7]. Otherwise stated, thermal energy is not involved in the origins of magnetisation of a permanent magnet. On the contrary, as the temperature decreases towards absolute zero, the stronger will be the magnetic field created by a permanent magnet [8].

It is forecasted by Quantum Field Theory [9] that the free space implicitly has a vastly complex structure. All of the properties that a particle may have (like spin, or polarization in the case of light, energy, and so on) are present at each and every point in space, like in a chaotic "sea of activity". On average, all these superimposed properties cancel out, and the free space is, after all, empty in this sense.

Moreover, electrons could perform the interface for converting chaotic energy in free space to useful energy on a macroscopic scale [10]. In particular, the magnetization activity in a permanent magnet would be an example of a continuously on-going energetic process fed by the random energy of the free space. According to [10], the underlying reason why in an atomic structure electrons (negative charge) do not collapse to protons (positive charge) is because the electrons underway to the otherwise expected collision catch energy from photons (particles without mass and charge) present in the free space, being therefore repulsed back from the protons. After that, energy is released from the electrons to the free space again in the form of photons. So, the stability of the atoms would be due to the persistent interaction of electrons with the chaotic energy in free space.

In the case of permanent magnets, since the circulation of electrons in the atomic structure is in joint synchronism, with all magnetic moments oriented in the same direction, the photons that are incessantly released back to the free space would then create collectively a coherent pattern in the space around the magnet, which builds up the magnetic field (vector \vec{B} in (2)), as characterized by closed

magnetic flux lines. And so, one magnet would "feel" the force of another one in its proximity.

The closed current filaments with linear wires in Fig. 1 can be considered elementary models of permanent magnets. As long as current circulates in the loops, the magnetic field will be maintained in space, and there will be forces actuating on the wires. On account of the fundamental analytical equations in Section 3, it is forecasted that a quirky rotation of the loops unfolds useful mechanical energy. In this case, the primary source of energy, the one that keeps the constant currents permanently circulating in the loops (generating magnetic moments in this way), would be the "sea of activity", the chaotic energy in the free space. Having said that, the excess energy found in (22) is not in contradiction with any of the Three Laws of Thermodynamics [11].

5 Conclusion

The presented model for the phenomena claimed in [1] follows an engineering approach, in the sense that essentially "*all models are wrong, but some are useful*" [12]. The accompanying analytical equations are an invitation to try other shapes or combinations of (multiple) current loops with synchronized (or not) relative displacements among them, aiming at discovering other possible geometries that, in theory, yield energy in abundance. But it remains a valid research question: can the proposed model be of some value for the synthesis of working prototypes, or is there something fundamentally wrong with it?

Acknowledgements

The author would like to thank L. Kurmann for sharing the results in [3] and for the valuable discussions.

As an aside, circular current loops can also represent elementary cylindrical electromagnets.

Appendix A

A general formula for calculating the magnetic force between inclined circular loops is presented in [6]. In the case of the geometry considered in Fig.1, for given inclination angle ϕ , after some manipulations the force components in (8) actuating on the secondary current loop are found to become

$$\vec{F}_S = F_x \vec{a}_x + F_y \vec{a}_y + F_z \vec{a}_z$$

with

$$\begin{aligned} F_x &= \frac{\mu_0 I_P I_S R_S}{8\pi\sqrt{R_P}} \int_0^{2\pi} I_x d\varphi, \\ F_y &= \frac{\mu_0 I_P I_S R_S}{8\pi\sqrt{R_P}} \int_0^{2\pi} I_y d\varphi, \\ F_z &= \frac{\mu_0 I_P I_S R_S}{8\pi\sqrt{R_P}} \int_0^{2\pi} I_z d\varphi, \end{aligned} \quad (27)$$

where

$$\begin{aligned} I_x &= \frac{k}{(x_S^2 + y_S^2)^{5/4}} \left[z_S y_S \ell_{S_z} L_0 + \sqrt{x_S^2 + y_S^2} \ell_{S_y} S_0 \right], \\ I_y &= \frac{k}{(x_S^2 + y_S^2)^{5/4}} \left[z_S x_S \ell_{S_z} L_0 + \sqrt{x_S^2 + y_S^2} \ell_{S_x} S_0 \right], \\ I_z &= \frac{k}{(x_S^2 + y_S^2)^{5/4}} z_S [x_S \ell_{S_y} - y_S \ell_{S_x}], \end{aligned} \quad (28)$$

and

$$\begin{aligned} k^2 &= \frac{4R_P \sqrt{x_S^2 + y_S^2}}{\left(R_P + \sqrt{x_S^2 + y_S^2}\right)^2 + z_S^2}, \\ K(k) &= \int_0^{\pi/2} \frac{1}{\sqrt{1 - k^2 \sin^2 \xi}} d\xi, \\ E(k) &= \int_0^{\pi/2} \sqrt{1 - k^2 \sin^2 \xi} d\xi, \\ L_0 &= 2K(k) - \frac{2 - k^2}{1 - k^2} E(k), \\ S_0 &= 2\sqrt{x_S^2 + y_S^2} K(k) + \frac{2\sqrt{x_S^2 + y_S^2} - \left(R_P + \sqrt{x_S^2 + y_S^2}\right) k^2}{1 - k^2} E(k). \end{aligned} \quad (29)$$

Further,

$$\begin{aligned} \ell_{S_x} &= -\cos \phi \cos \varphi, \\ \ell_{S_y} &= -\sin \varphi, \\ \ell_{S_z} &= \sin \phi \cos \varphi, \end{aligned} \quad (30)$$

and

$$\begin{aligned}x_S &= x_C - R_S \cos \phi \sin \varphi, \\y_S &= y_C + R_S \cos \varphi, \\z_S &= z_C + R_S \sin \phi \sin \varphi,\end{aligned}\tag{31}$$

or

$$\begin{aligned}x_S &= r_S \sin \phi - R_S \cos \phi \sin \varphi, \\y_S &= A_0 + A_S \sin \phi + R_S \cos \varphi, \\z_S &= -r_P + r_S \cos \phi + R_S \sin \phi \sin \varphi,\end{aligned}\tag{32}$$

since x_C, y_C and z_C are defined in (13), (14) and (15), respectively.

Appendix B

```

%%%%%%%%%%%%%%%%%%%%%%%%%%%%%%%%%%%%%%%%%%%%%%%%%%%%%%%%%%%%%%%%%%%%%%%%
%
% Main function: Joule_1x2Loops
%
% Analytical description of the energy related to
% the magnetic torque and force as developed by
% 1 SET of TWO current-carrying circular loops
% placed on concentric cylindrical surfaces
%
% Accompanying functions : Joule_2Loops.m & TorqueForce_2Loops.m;
%
%-----
% jduarte @ July 22, 2018
%-----

% Parameters: Primary (stator) and Secondary (rotor) circular loops -----
par.IP = -1; par.IS = 1;           % loop currents; mind the polarity!
par.RP = 5e-3; par.RS = 5e-3; % inner radii
par.rP = 30e-3;                   % perpendicular distance to the zz-axis
par.rS = 25e-3;                   % perpendicular distance to the zz-axis
par.AS = 17e-3;                   % amplitude of harmonic displacement
par.A0 = 9.5e-3;                  % offset displacement turning point
par.steps = 1000;                 % integration steps (should be multiple of 2)
%
par.Fpu = 1e-9;                   % normalization of forces in nN
%-----

% Main reference frame: xx-, yy-, zz- orthogonal axes -----
% - Two concentric cylindrical surfaces along zz-axis
% - Prim- and sec- loops are placed on the cylindrical surfaces
% -- therefore with loop normal vectors perpendicular to the zz-axis
% phiP : inclination of prim-loop normal vector w.r.t. zz-axis
% phiS : inclination of sec-loop normal vector w.r.t. zz-axis
% zzP  : longitudinal position of center prim-loop in the zz-axis
% zzS  : longitudinal position of center sec-loop in the zz-axis
% thetaS : angle used for calculating cam displacement along zz-axis
%

```

```

% Initial cylindrical placement of the loops
% -- inclination of prim and sec normal-vectors w.r.t. zz-axis
phiP0 = 0;  phiS0 = 0;
% -- longitudinal position of center prim- and sec-loops on the zz-axis
zzP0 = 0;  zzS0 = par.A0;
%-----

% Interaction between loops -----
%   phiS_ : array (of par.steps) with rotation angles  $0 < \phi_S < 2\pi$ 
%   Tzz_ : array with normalized torques corresponding to phiS_
%   Fzz_ : array with normalized torques corresponding to phiS_
% -----
[phiS_,jTzz_,jFzz_] = Joule_2Loops(phiS0,phiP0,zzS0,zzP0,par);
%
%-----

% Total energy requirement -----
JouleTzz = sum(jTzz_),
JouleFzz = sum(jFzz_),
JouleS   = JouleTzz +JouleFzz,
%-----

% Show energy incrementals as function of radial position sec-loop -----
x =phiS_/pi -1; % normalized horizontal axis from  $-\pi < \phi_S < \pi$ 
y1 = zeros(1,par.steps); y2 =zeros(1,par.steps);
for i =1:par.steps/2
y1(i) =jTzz_(i+par.steps/2); y1(i+par.steps/2) =jTzz_(i);
y2(i) =jFzz_(i+par.steps/2); y2(i+par.steps/2) =jFzz_(i);
end
y3 = y1 +y2; % netto energy
%
figure(1)
plot(x,y1,'--k',x,y2,'-.k',x,y3,'-k','LineWidth',1);
title('Energy incrementals','Interpreter','latex');
xlabel('$\phi / \pi$', 'Interpreter','latex');
ylabel('$dQ / nJ$', 'Interpreter','latex');
legend({'$dQ_{\phi}$','$dQ_y','$dQ_{\Sigma}$'},...
'Interpreter','latex','FontSize',10);
grid on;

%
% end main function: Joule_1x2Loops -----

```

```

%%%%%%%%%%%%%%%%%%%%%%%%%%%%%%%%%%%%%%%%%%%%%%%%%%%%%%%%%%%%%%%%%%%%%%%%%%%%%%
%
function [phiS_,jTzz_,jFzz_] = Joule_2Loops(phiS0,phiP0,zzS0,zzP0,par)
% 2 loops perpendicular to the zz-axis
% Incremental Joule when sec-loop is translated by increments (0<phiS<2*pi)
% and axially displaced (0<thetaS<2*pi) at the same time
%
% Accompanying function : TorqueForce_2Loops.m
%
%-----
% jduarte @ July 22, 2018
%-----

% Loop parameters -----
% par.IP ; par.IS; % Amp
% par.RP ; par.RS; % Own radii
% par.rP ; par.rS % radial distances perpendicular to the zz-axis
AS=par.AS; % amplitude of cam displacement along the zz-axis

% Main reference frame: ortogonal xx-, yy-, zz- axes -----
% - Two cylidrical surfaces concentric along zz-axis
% - Primary and secondary loops are placed on the cylindrical surfaces
% -- therefore with loop normal vectors perpendicular to the zz-axis
% phiP : inclination of prim-loop normal vector w.r.t. zz-axis
% phiS : inclination of sec-loop normal-vector w.r.t. zz-axis
% zzP : longitudinal position of center prim-loop in the zz-axis
% zzS : longitudinal position of center sec-loop in the zz-axis
% thetaS : angle used for calculating cam displacement along zz-axis

% initial conditions -----
thetaS =0; phiS =phiS0; phiP =phiP0; zzP =zzP0;
phiS_ = []; jTzz_ = []; jFzz_ = []; % recording arrays

% calculations -----
k =0; % counter for display of calculations on-the-fly
dS = 2*pi/par.steps; % incremental value for phiS and thetaS
for i=1:par.steps % qsiS and phiS <= 2*pi,
%
phiS = phiS +dS; % increase inclination angle
%
thetaS = thetaS +dS; % increase angle for axial displacement
zzS = zzS0+AS*sin(thetaS); % turning point absolute location
dzzS = AS*cos(thetaS)*dS; % limit case differential displacement
%

```

```

[Tzz,Fzz] = TorqueForce_2Loops(phiS,zzS,phiP,zzP,par);
jTzz = Tzz*dS;    % energy increment due to torque (circunf force)
jFzz = Fzz*dzzS;  % energy increment due to axial force
%
% register
phiS_ = [phiS_,phiS];
%phiS_ = [phiS_,thetaS]; % when showing only axial displacements
jTzz_ = [jTzz_,jTzz]; jFzz_ = [jFzz_,jFzz];
%
k =k+1;
if mod(k,100) == 0, fprintf(''); end % visualization
%
end % while

fprintf('\n');
end % function Joule_2Loops -----

```

```

%%%%%%%%%%%%%%%%%%%%%%%%%%%%%%%%%%%%%%%%%%%%%%%%%%%%%%%%%%%%%%%%%%%%%%%%%%%%%%
%
function [Tzz,Fzz] = TorqueForce_2Loops(phiS,zzS,phiP,zzP,par)
% According to
%   S. Babic & C. Aykel;"Magnetic Force between Inclined Circular Loops
%   (Lorentz approach); Progress in Electromagnetic Research B, Vol. 38,
%   333-349, 2012.
%
%-----
% jduarte @ July 22, 2018
%-----

% Main reference frame:  xx-, yy-, zz- orthogonal axes -----
% - Two concentric cylindrical surfaces along the zz-axis
% - Prim- and sec- loops are placed on the cylindrical surfaces
% -- therefore with loop normal-vectors perpendicular to the zz-axis
% phiP = inclination of prim-loop normal vector w.r.t. zz-axis
% phiS = inclination of sec-loop normal vector w.r.t. zz-axis
% zzP  = longitudinal position of center prim loop in the zz-axis
% zzS  = longitudinal position of center sec loop in the zz-axis

% Loop parameters -----
IP = par.IP;  IS = par.IS; % Amp
RP = par.RP;  RS = par.RS; % Inner radii
rP = par.rP;  rS = par.rS; % radial distances perpendicular to the zz-axis
Fpu = par.Fpu; % normalization of force values to nN

% Prim-loop creates reference frame XYZ with i-, j-, k- unity vectors ---
% - i-vector in the loop plane and perpendicular to zz-axis
% - j-vector in the loop plane and parallel to zz-axis
% - k-vector normal to the loop and perpendicular to zz-axis
%
% Prim-loop placed at plane XOY (Z=0) -----
% - axis of X parallel to i-vector
% - axis of Y parallel to j-vector (and also parallel to zz-axis)
% - axis of Z parallel to k-vector
% - prim loop centered at 0(x=0,y=0,z=0)

% Sec-loop with coordinates referenced to XYZ -----
% - sec-loop normal vector: a*i +b*j + c*k, with b=0
% --- with center at: C(xC, yC, zC)
% --- and a point on the loop circle: DS(x0, y0, z0)
% --- loop plane: a*x +b*y +c*z +D = 0

```

```

% Parameters sec loop with reference to XYZ -----
%
% angle inclination of sec-loop normal vector w.r.t. the k-vector
phi = phiS -phiP;
% -- sec-loop normal vector :  $N = \sin(\phi)i + 0*j + \cos(\phi)k$  with
% -- sec-loop with center at:  $C(xC, yC, zC)$ 
xC = rS*sin(phi);
yC = zzS-zzP;
zC = rS*cos(phi) -rP;
%
% Plane of sec-loop w.r.t. XYZ frame -----
% --- :  $\sin\phi(x-xC) + 0*(y-yC) + \cos\phi(z-zC) = 0$ 
% --- :  $a*x + b*y + c*z + D = 0$ 
% --- :  $\sin(\phi)*x + 0*y + \cos(\phi)*z + D = 0$ 
a = sin(phi); b = 0; c = cos(phi); D = rP - rS;
%
% Sec loop unit vectors w.r.t. XYZ frame -----
%  $N = (nx, ny, nz)$   $u = (ux, uy, uz)$   $v = (vx, vy, vz)$ 
L = sqrt(a^2 + b^2 + c^2); l = sqrt(a^2 + c^2);
nx = a/L;      ny = b/L; nz = c/L;
ux = -a*b/(l*L); uy = l/L; uz = -b*c/(l*L);
vx = -c/l;     vy = 0;   vz = a/l;
%-----

% Force components on the sec-loop w.r.t. the prim-loop i-, j-, k-vectors
mu0 = 4*pi*1e-7;
F = mu0*IP*IS*RS/(8*pi*sqrt(RP))/Fpu; % normalization
%
% Integration around  $0 < \phiS < 2\pi$  / analytical -----
Fx = F*integral(@(w)Ix(w),0,2*pi);
Fy = F*integral(@(w)Iy(w),0,2*pi);
Fz = F*integral(@(w)Iz(w),0,2*pi);
%
%-----

% Tangential force in sec-loop w.r.t. zz-axis (= normal to j-vector) --
Ft = Fx*cos(phi) + Fz*cos(phi+pi/2);
%
% Resulting torque/force components w.r.t. zz-axis -----
Tzz = Ft*rS; % torque around zz-axis
Fzz = Fy;    % longitudinal force along the zz-axis
%-----
%
% end TorqueForce_2Loops -----

```

```

%-----
% Local Functions
%

function h = Ix(theta) % -----
%
costheta =cos(theta); sintheta =sin(theta);
%
xS = xC +RS.*ux.*costheta +RS.*vx.*sintheta;
yS = yC +RS.*uy.*costheta +RS.*vy.*sintheta;
zS = zC +RS.*uz.*costheta +RS.*vz.*sintheta;
xyS = sqrt(xS.^2 +yS.^2);
%
lSx = -ux.*sintheta +vx.*costheta;
lSy = -uy.*sintheta +vy.*costheta;
lSz = -uz.*sintheta +vz.*costheta;
%
% elliptic integrals
k2 = 4.*RP.*xyS./((RP+xyS).^2 +zS.^2); k =sqrt(k2);
[K,E] = ellipke(k2); % 1- and 2-order complete elliptic integrals
L0 = 2.*K - E.*(2-k2)./(1-k2);
S0 = 2.*xyS.*K - E.*(2.*xyS -(RP +xyS).*k2)./(1-k2);
%
% Integrands
kk = k./(xS.^2+yS.^2).^(5./4);
h = kk.*(zS.*yS.*lSz.*L0 +xyS.*lSy.*S0);
% Ix = kk*(zS*yS*lSz*L0 +xyS*lSy*S0);
% Iy = -kk*(zS*xS*lSz*L0 +xyS*lSx*S0);
% Iz = kk*zS*(xS*lSy -yS*lSx)*L0;
%
end % Ix -----

function h = Iy(theta) %-----
%
costheta =cos(theta); sintheta =sin(theta);
%
xS = xC +RS.*ux.*costheta +RS.*vx.*sintheta;
yS = yC +RS.*uy.*costheta +RS.*vy.*sintheta;
zS = zC +RS.*uz.*costheta +RS.*vz.*sintheta;
xyS = sqrt(xS.^2 +yS.^2);
%
lSx = -ux.*sintheta +vx.*costheta;
lSy = -uy.*sintheta +vy.*costheta;
lSz = -uz.*sintheta +vz.*costheta;

```

```

%
% elliptic integrals
k2 = 4.*RP.*xyS./((RP+xyS).^2 +zS.^2); k =sqrt(k2);
[K,E] = ellipke(k2);
L0 = 2.*K - E.*(2-k2)./(1-k2);
S0 = 2.*xyS.*K - E.*(2.*xyS -(RP +xyS).*k2)./(1-k2);
%
% Integrands
kk = k./(xS.^2+yS.^2).^(5./4);
h = -kk.*(zS.*xS.*lSz.*L0 +xyS.*lSx.*S0);
% Ix = kk*(zS*yS.*lSz.*L0 +xyS.*lSy.*S0);
% Iy = -kk*(zS*xS.*lSz.*L0 +xyS.*lSx.*S0);
% Iz = kk*zS*(xS.*lSy -yS.*lSx).*L0;
%
end % Iy -----

function h = Iz(theta) %-----
%
costheta =cos(theta); sintheta =sin(theta);
%
xS = xC +RS.*ux.*costheta +RS.*vx.*sintheta;
yS = yC +RS.*uy.*costheta +RS.*vy.*sintheta;
zS = zC +RS.*uz.*costheta +RS.*vz.*sintheta;
xyS = sqrt(xS.^2 +yS.^2);
%
lSx = -ux.*sintheta +vx.*costheta;
lSy = -uy.*sintheta +vy.*costheta;
lSz = -uz.*sintheta +vz.*costheta;
%
% elliptic integrals
k2 = 4.*RP.*xyS./((RP+xyS).^2 +zS.^2); k =sqrt(k2);
[K,E] = ellipke(k2);
L0 = 2.*K - E.*(2-k2)./(1-k2);
S0 = 2.*xyS.*K - E.*(2.*xyS -(RP +xyS).*k2)./(1-k2);
%
% Integrands
kk = k./(xS.^2+yS.^2).^(5./4);
h = kk.*zS.*(xS.*lSy -yS.*lSx).*L0;
% Ix = kk*(zS*yS.*lSz.*L0 +xyS.*lSy.*S0);
% Iy = -kk*(zS*xS.*lSz.*L0 +xyS.*lSx.*S0);
% Iz = kk*zS*(xS.*lSy -yS.*lSx).*L0;
%
end % Iz -----
%
```

```
% end Local Functions
```

%

%%%%%%%%%%%

References

- [1] M. Yildiz; *Device having an arrangement of magnets*; WO 2009/019001 A3.
- [2] J.L. Duarte; *Introducing the Yildiz Motor & Modeling the Yildiz Motor*; in Non-patent literature (EZ81K3II8231020) cited during the examination procedure of Application No. 08801521 with reference to "EP2153515 Device Having an Arrangement of Magnets" by M. Yildiz; WIPO Patent Collections, 2017.
- [3] L. Kurmann and Y. Jia; *Oscillators with Nonpolar Magnetic Repulsion System and its Use in Rotary Nonresonant and Resonant Kinetic Energy Harvesters*; May 2018, private communication.
- [4] J.A. Stratton; *Electromagnetic Theory*; McGraw Hill, 1941.
- [5] E. Durand; *Magnétostatique*; Masson et Cie., 1968.
- [6] A. Babic and C. Aykel; *Magnetic force between inclined circular loops (Lorentz approach)*; Progress In Electromagnetics Research B, Vol. 38, 333-349, 2012.
- [7] B.D. Cullit and C.D. Graham; *Introduction to Magnetic Materials*, 2nd ed.; Wiley, 2009.
- [8] Z. Abdelnour, H. Mildrum, and K. Strnat; *Properties of various sintered rare earth-cobalt permanent magnets between -60° and $+200^{\circ}$ C*; IEEE Transactions on Magnetics; Vol.16, No.5, 994-996, Sep. 1980.
- [9] R.P. Feynman; *Quantum Electrodynamics*; Westview Press, 1998.
- [10] H. Puthoff; *Ground state of hydrogen as a zero-point-fluctuation-determined state*; Phys. Rev. D, vol. 35, no. 10, 1987.
- [11] E. Fermi, *Thermodynamics*, Dover Publications Inc., 1936.
- [12] G. Box, *Robustness in the strategy of scientific model building*, in R.L. Launer and G.N. Wilkinson, "Robustness in Statistics", Academic Press, pp. 201236, 1979.

J.L. Duarte
Eindhoven, July 22nd, 2018

Modeling the Yildiz Motor revisited

Addendum

After peer review, the *strict* answer to the research question as formulated in the Conclusion:

"Can the proposed model be of some value for the synthesis of working prototypes, or is there something fundamentally wrong with it?"

would be the latter is true.

The reasons why is that the *total* magnetic force, as created by one current loop on the other loop, has been assumed concentrated on the loop geometric center in order to derive the torque arm. As a consequence, energy excess appears at each revolution of the loops. However, if the torque is calculated incrementally, by integrating *local* forces acting on incremental current loop segments, the energy excess will be found to become zero.

Nevertheless, the software used in [3] for torque calculations through FEM (COMSOL Multiphysics) also brings about similar torque asymmetry with, consistently, a small average value different from zero. Is it due to numerical inaccuracy? Which modifications are then necessary in order to obtain reliable results?

The proposed design method is therefore uncertain. Yet, if the loops are suppose to model (imaginary) Amperian currents on the surface of PMs, the spatial position of the current loop segments is rather a mathematical abstraction without physical meaning. Hence, a new question arises: is it accurate to consider a torque arm based on the *local* position of fictitious currents?

First appeared: March 15th, 2019

This version: April 22nd, 2019

J.L. Duarte